AN EFFICIENT GAUSSIAN COLLOCATION METHOD FOR SOLVING DELAY VOLTERRA INTEGRO-DIFFERENTIAL EQUATIONS OF PANTOGRAPH TYPE

M. GHORBANZADEH* AND O. R. N. SAMADI

Departmant of Mathematics, Imam Reza International University, Mashhad, Iran

Abstract. This paper presents a new radial basis collocation method to obtain the approximate solution and approximate derivative of the solution for pantograph Volterra integro-differential equations. The method is based on an explicit interpolation formula of Gaussian radial basis functions. The proposed technique provides a simple, efficiant and stable algorithm which yields accurate resultls. Numerical experiments are included and the results are compared with analytical solution and with those of standard radial basis collocation method and spectral method to confirm the accuracy and efficiency of the new scheme.

1. Intorduction

Radial basis functions (RBFs) have been considered for solving partial differential equations in three decades ago [1, 2, 3]. They are appropriate choice to more traditional methods such as finite differences and finite elements methods. Part of their attractiveness returns to the fact that without orthogonality and complicated forms of other interpolants, it is able to approximate the functions with high(exponential) accuracy and fast rate of convergence [1]. Some other practical interests in RBFs methods are due to: (i) ability to handle data in multiple dimensions; (ii) flexibility in the node and centers locations; (iii)They are truly meshless methods; (iv) The RBFs collocation points can be defined with any interval because RBFs are defined in the whole real line [4]. However there have been some challenges with RBFs approaches. In their standard formulation, RBFs methods often involve the solution

2010 *Mathematics Subject Classification.* Primary 47A55; Secondary 39B52, 34K20, 39B82.

Key words and phrases. Radial basis function, shape parameter, meshless method.

* corresponding author:ghorbanzadeh_imamreza@yahoo.com

of linear systems whose system matrices usually are full and severely ill-conditioned, specially, if certain popular RBFs such as Gaussians or inverse multiquadrics are used with small values of their associated shape parameter. To be more precise, the challenges as mentioned in [5] are: serious numerical ill-conditioning for a fixed N (the number of collocation points or basis functions) and small shape parameter, similar ill-conditioning problems for a fixed shape parameter and large N. Also in [6] it has been proved that, if the shape parameter tends to zero then RBFs interpolation is equivalent to polynomial interpolation on the same nodes; hence in such a flat limit case the RBFs approximation suffers of Rung phenomenon. Some of various techniques which have been done to deal with the above difficulties include changing the basis of the approximation space, using techniques from complex analysis , applying contour-integral approach and using specialized preconditioners to the system matrix, see [7, 8] and references therein. In [9] the authors exploited a connection between Gaussian RBFs (GRBFs) and polynomials using standard tools of potential theory which provides a simple explicit interpolation formula through the use of some cardinal functions, so the difficulty of inverting the associated matrix can be avoided. Furthermore they obtained stable nodes that can prevent the Runge phenomenon and enable stable approximations.
It is only recently that the integral equations have been considered with the standard RBFs methods [10, 11, 12]. In contrast collocation schemes have been investigated for solving the delay integral and differential equations for a long time [13, 14, 15, 16, 17, 18, 19, 20]. To our best of knowledge nobody accomplished solving the delay Volterra integro-differential equations of pantograph type with a RBFs collocation method. This paper considers the following Pantograph Volterra Integro-Differential Equation (PVIDE) in bounded domain

$$y'(t) = g(t) + a(t)y(t) + b(t)y(qt) + \int_0^t K_0(t,s)y(s)ds + \int_0^{qt} K_1(t,s)y(s)ds, \quad t \in [0,T], \quad 0 < q < 1, \tag{1.1}$$

$$y(0) = \bar{y}_0, \tag{1.2}$$

For implementation of a high accuracy RBFs method, we assume the functions $a(t)$, $b(t)$, $g(t)$, $K_0(t,s)$ and $K_1(t,s)$ to be sufficiently smooth on their domains.
The PVIDEs are models of evolutionary problems with memory and have many applications such as the population dynamics, infectious diseases and chemical kinetics (see, e.g. , [21] and references therein).

Also to study the existence, uniqueness and regularity of solutions of (1.1) and (1.2), see [15].
There are some existing numerical methods for PVIDEs. In [22] the authors proposed a collocation method using piecewise polynomials, and analyzed the global and local orders of superconvergence of the collocation solutions for (1.1) and (1.2). Also in [23] the author applied a Legendre spectral method and analyzed the exponential convergence of the method where K_0 and K_1 are convolution. Our aim throughout this paper is to establish some results of the paper [9] on the $[0, T]$, specially the Gaussian RBF (GRBF) explicit interpolation formula. Then by employing of these results we offer a new Gaussian collocation method (NGCM) to approximate the solutions of the PVIDEs (which are often stiff and have oscillation on the related domain) and their first derivatives. Also we analyze how the problem parameters q and T and the parameters in our method i.e. N (number of basis functions or collocation points) and the shape parameter should be selected and how susceptible the approximations are to changes in the parameters. In addition in order to challenge the NGCM, we compare with the standard RBFs collocation methods and a spectral collocation method [24].
The following sections of this paper are structured as follows: in section 2 we describe the properties of radial basis functions and establish the GRBF explicit interpolation formula. The NGCM is implemented in section 3. To support our findings, we present results of numerical experiments in section 4. The conclusions are discussed in the final section.

2. Basic knowledge about RBFs

In this section, we collect some well-known definitions and properties from [9, 25] which we shall utilize throughout the paper.

Definition 2.1. Let Π_m denotes the subspace of $C(\mathbb{R}^d)$ consisting of all algebraic polynomials of degree less than m on $\mathbb{R}^d$ and $\phi : \mathbb{R}^d \to \mathbb{R}$ be a continuous function. We say that ϕ is conditionally positive definite of order $m \in \mathbb{N}$ if for every finite set of pairwise distinct points $X = \{\xi_1, \cdots, \xi_N\} \subseteq \mathbb{R}^d$ and for every $\alpha = (\alpha_1, \cdots, \alpha_N) \in \mathbb{R}^N \setminus 0$ satisfying

$$\sum_{j=1}^{N} \alpha_j p(\xi_j) = 0, \quad p \in \Pi_m,$$

the quadric form

$$\sum_{i=1}^{N}\sum_{j=1}^{N}\alpha_i\alpha_j\phi(\xi_i-\xi_j)$$

is positive definite.

Definition 2.2. A function $\phi : \mathbb{R}^d \to \mathbb{R}$ is radial in the sense that $\phi(t) = \varphi(r)$, where $r = \|t\|$ and $\|\cdot\|$ is the usual Euclidean norm.
RBFs fall into two main classes: infinitely smooth and including a free parameter (shape parameter), such as multiquadrics ($\varphi(r) = \sqrt{r^2+c^2}$) and Gaussians ($\varphi(r) = e^{-\frac{r^2}{c^2}}$); and piecewise smooth and parameter free, such as cubics ($\varphi(r) = r^3$) and thin plate splines ($\varphi(r) = r^2 \ln r$).

2.1. **Standard RBF (SRBF) interpolation.** Let $f : \mathbb{R}^d \to \mathbb{R}$ be a continuous function and given a set of distinct points(centers)
$X = \{\xi_0, \cdots, \xi_N\}$ in $\Omega \subseteq \mathbb{R}^d$. Interpolation of f on X using RBFs usually takes the following form

$$I_N f = \sum_{n=0}^{N}\lambda_n\phi(t-\xi_n) + \sum_{m=1}^{l}\alpha_m p_m(t), \tag{2.1}$$

where $\{p_m\}_{m=1}^{l}$ is a basis for Π_M and $\lambda's$ and $\alpha's$ are coefficients to be determined.
Equation of (2.1) can be written without the additional polynomial term. In that case ϕ must be unconditionally positive definite to ensure the solvability of the resulting system. (e.g. Gaussian or inverse multiquadric) [26]. Hence (2.1) can be presented as follow

$$I_N f = \sum_{n=0}^{N}\lambda_n\phi(t-\xi_n), \tag{2.2}$$

Let the expansion coefficient vector λ be $\lambda = [\lambda_0, \cdots, \lambda_n]^T$ then from interpolation conditions $I_N f(t_n) = f(t_n)$, $n = 0, \cdots, N$ we reach a system of linear equations that can be displayed in matrix form as

$$\Phi\lambda = F, \tag{2.3}$$

where $F = [f(t_0), \cdots, f(t_N)]^T$, $\Phi_{ij} = \phi(t_i - \xi_j)$ and $\{t_i\}_{i=0}^{N}$ are the interpolation points.
Note that for all infinitely smooth RBFs the coefficient matrix Φ in (2.3) is nonsingular [1]. So the unique interpolant of the form (2.2) can be obtained.

2.2. **New GRBFs interpolation.** For providing an explicit interpolation formula based on the GRBFs in (2.2) we choose $d = 1$ and centers $\xi_n = hn,\ n = 0, 1, \cdots, N,\ h = \frac{T}{N}$ on $[0, T]$. Therefor the GRBF approximation is

$$I_N f = \sum_{n=0}^{N} \lambda_n e^{-\left(\frac{t-hn}{c}\right)^2} = e^{-\frac{t^2}{c^2}} \sum_{n=0}^{N} \lambda_n e^{-\frac{h^2 n^2}{c^2}} e^{\frac{2tnh}{c^2}}, \tag{2.4}$$

following [9], we let $\beta = \frac{2h}{c^2} = \frac{2T}{Nc^2}$ and apply the transformation

$$s = e^{\beta t}, \quad s \in [1, e^{\beta T}],$$

to find that

$$G(s) = I_N f\big(\frac{\log s}{\beta}\big) = e^{-\frac{N \log^2 s}{2T\beta}} \sum_{n=0}^{N} \tilde{\lambda}_n s^n = \psi_\beta^N(s) \sum_{n=0}^{N} \tilde{\lambda}_n s^n, \tag{2.5}$$

Where the $\lambda' s$ are independent of s.
From (2.5) it is clear that $\frac{G}{\psi_\beta^N}$ is a polynomial of degree no greater than N. If F is chosen by interpolation to a given f at $N + 1$ points, then we have following theorem in the complex plane $z = t + iy$.
Theorem: suppose that f is analytic in a closed simply connected region R that lies inside the strip $-\frac{\pi}{2\beta} < \mathrm{Im}(z) < \frac{\pi}{2\beta}$ and that C is simple, closed and rectifiable curve that lies in R and contains the interpolation points $t_0, t_1, \cdots, t_N$. Then the remainder of the GRBF interpolation for f at t can be represented as the contour integral

$$f(t) - I_N f(t) = \frac{\beta \eta_N(t)}{2\pi i} \int_C \frac{f(z) e^{\beta z}}{\eta_N(z)(e^{\beta z} - e^{\beta t})} dz,$$

where

$$\eta_N(t) = e^{-\frac{N\beta}{2T} t^2} \prod_{k=0}^{N} (e^{\beta t} - e^{\beta t_k}).$$

Proof. Consider the conformal map $w = e^{\beta z}$ and let $g(s) = f\big(\frac{\log s}{\beta}\big)$. Under this transformation, the region R is mapped to a closed simply connected region that lies in the half-plane $\mathrm{Re}(w) > 0$. Thus $\frac{g}{\psi_\beta^N}$ is analytic in this region in the w-plane, and we can use the Hermite formula for the error in polynomial interpolation [27],

$$\begin{aligned} g(s) - G(s) &= \psi_\beta^N(s)\big(\frac{g(s)}{\psi_\beta^N(s)} - \sum_{k=0}^{N} \tilde{\lambda}_k s^k\big) \\ &= \frac{\psi_\beta^N(s) \prod_{k=0}^{N}(s - s_k)}{2\pi i} \int_{\mathcal{C}} \frac{g(w)}{(w - s)\psi_\beta^N \prod_{k=0}^{N}(w - s_k)} dw, \end{aligned}$$

where $s_k = e^{\beta t_k}$ and $\mathcal{C}$ is the image of C in the w-plane. A change of variables completes the proof. □

Using above theorem and if we let μ be the limiting node density function [28] of nodes on$[0,T]$ and defining the logarithmic potential function as follow

$$\mu_\beta(z) = \frac{\beta}{2T}\mathrm{Re}(z^2) - \int_0^T \log(|e^{\beta z} - e^{\beta t}|)\mu(t)dt,$$

similar to [9] by applying standard potential theory one can prove that the GRBF interpolant converges exponentially to the target function on $[0,T]$ under some conditions.
Now we define an explicit interpolation formula through the following Gaussian cardinal functions

$$L_n(t) = e^{-\frac{N\beta}{2T}(t^2-t_n^2)} \prod_{\substack{j=0 \\ j\neq n}}^{N} \frac{e^{\beta t} - e^{\beta t_j}}{e^{\beta t_n} - e^{\beta t_j}}, \tag{2.6}$$

It is easy to verify that $L_n(t_n) = 1,\ L_n(t_j) = 0,\ j \neq n$ and by (2.5), $L_n(t) \in \mathrm{span}\{e^{-\frac{(t-\xi_n)^2}{c^2}}\}$. So we can write the unique GRBF interpolant as

$$I_N f(t) = \sum_{n=0}^{N} f(t_n)L_n(t), \tag{2.7}$$

3. New Gaussian collocation method (NGCM)

Consider the PVIDE given in (1.1) and (1.2). At first, for ease of applying the NGCM we restate the initial condition (1.2) as

$$y(t) = y_0 + \int_0^t y'(s)ds, \tag{3.1}$$

so without integration both sides of (1.1) one can approximate the $y(t)$ and $y'(t)$ using the NGCM naturally. This idea has been used in some literature [24, 29].
In order to acquire a computationally form of the collocation equations (1.1) and (3.1), we declare y_N and y'_N on $[0,T]$ by (2.7) as

$$y_N = I_N y(t) = \sum_{k=0}^{N} y_k L_k(t), \quad y_k = y(t_k), \tag{3.2}$$

$$y'_N = I_N y'(t) = \sum_{k=0}^{N} y'_k L_k(t), \quad y'_k = y'(t_k), \tag{3.3}$$

with

$$L_k(t) = \prod_{\substack{j=0 \\ j\neq k}}^{N} = \frac{e^{-\frac{\beta}{2T}(t^2-t_k^2)}(e^{\beta t} - e^{\beta t_j})}{e^{\beta t_k} - e^{\beta t_j}}, \quad k = 0, 1, \cdots, N, \tag{3.4}$$

which is a simple modification of (2.6) that improves the accuracy of approxmitions.

As on outcome of the above notations, the collocation equations (1.1) and (3.1) at the collocation points $\{t_i\}_{i=0}^N$ turn to

$$\begin{aligned} y_i' &= g(t_i) + a(t_i)y_i + b(t_i)y_N(qt_i) + \int_0^{t_i} K_0(t_i, s)y_N(s)ds + \\ &\int_0^{qt_i} K_1(t_i, s)y_N(s)ds \\ y_i &= y_0 + \int_0^{t_i} y_N'(s)ds, \quad i = 0, 1, \cdots, N. \end{aligned} \tag{3.5}$$

Now we change the integration intervals to $[0, T]$ using the following transformations

$$s = s_i(\theta) = \frac{t_i}{T}\theta, \quad s = s_i^q(\theta) = \frac{qt_i}{T}\theta.$$

Therefor the above equations become

$$\begin{aligned} y_i &= g(t_i) + a(t_i)y(t_i) + b(t_i)y_N(qt_i) + \frac{t_i}{T}\int_0^T K_0\big(t_i, s_i(\theta)\big)y_N\big(s_i(\theta)\big)d\theta \\ &+ \frac{qt_i}{T}\int_0^T K_1\big(t_i, qs_i(\theta)\big)y_N\big(qs_i(\theta)\big)d\theta, \\ y_i &= y_0 + \frac{t_i}{T}\int_0^T y_N'\big(s_i(\theta)\big)d\theta, \quad i = 0, 1, \cdots, N. \end{aligned} \tag{3.6}$$

After applying the (3.2) and (3.3) we have

$$\begin{aligned} y_i' &= g(t_i) + a(t_i)y_i + b(t_i)\sum_{k=0}^{N} L_k(qt_i)y_k + \frac{t_i}{T}\sum_{k=0}^{N}\Big(\int_0^T K_0\big(t_i, s_i(\theta)\big)L_k\big(s_i(\theta)\big)d\theta\Big)y_k \\ &+ \frac{qt_i}{T}\sum_{k=0}^{N}\Big(\int_0^T K_1\big(t_i, qs_i(\theta)\big)L_k\big(qs_i(\theta)\big)d\theta\Big)y_k, \\ y_i &= y_0 + \frac{t_i}{T}\sum_{k=0}^{N}\Big(\int_0^T L_k\big(s_i(\theta)\big)d\theta\Big)y_k', \quad i = 0, 1, \cdots, N. \end{aligned} \tag{3.7}$$

In order to acquire a succinct notation for the above linear algebraic equations, we introduce the matrices and vectors

$$\bar{Y}_N = [\bar{y}_0, \cdots, \bar{y}_0]^T, \quad Y_n = [y_0, \cdots, y_N]^T, \quad Y'_N = [y'_0, \cdots, y'_N]^T,$$
$$G_N = [g(t_0), \cdots, g(t_N)]^T,$$
$$D_N = \text{diagonal}\big(a(t_0), \cdots, a(t_N)\big), \quad A^q_{1,N} = \big(b(t_i)L_k(qt_i)\big)_{0\le i,k\le N},$$
$$A_{2,N} = \Big(\frac{t_i}{T}\int_0^T K_0\big(t_i, s_i(\theta)\big)L_k\big(s_i(\theta)\big)d\theta\Big)_{0\le i,k\le N},$$
$$A^q_{3,N} = \Big(\frac{qt_i}{T}\int_0^T K_1\big(t_i, qs_i(\theta)\big)L_k\big(qs_i(\theta)\big)d\theta\Big)_{0\le i,k\le N},$$
$$A_{4,N} = \Big(\frac{t_i}{T}\int_0^T L_k\big(s_i(\theta)\big)d\theta\Big)_{0\le i,k\le N}.$$

So the corresponding system of linear algebraic equations (3.7) take the following form

$$\begin{aligned} Y'_N &= G_N + (D_n + A^q_{1,N} + A_{2,N} + A^q_{3,N})Y_N, \\ Y_N &= \bar{Y}_N + A_{4,N}Y'_N. \end{aligned} \tag{3.8}$$

We expose (3.8) in a compact form as follow

$$\begin{bmatrix} B_N & -I_N \\ I_N & -A_{4,N} \end{bmatrix} \begin{bmatrix} Y_N \\ Y'_N \end{bmatrix} = \begin{bmatrix} -G_N \\ \bar{Y}_N \end{bmatrix}, \tag{3.9}$$

where $B_N = D_N + A^q_{1,N} + A_{2,N} + A^q_{3,N}$ and I_N denotes the identity matrix.

In this way, a linear algebraic system is acquired which can be solved with an appropriate method and yield the unknown vectors Y_N and Y'_N.

To accelerate solving the linear algebraic system (3.9) one can approximate the integral terms in (3.7) by a suitable and high accurate numerical integration method such as $(N+1)$-points Gauss-Legendre, Gauss-Radau or Gauss-Lobatto quadrature formula concerning the Legendre weight.

4. Numerical results

In this section, we consider two oscillatory PVIDEs, to verify the performance of the NGCM. We numerically investigate how the selection of the parameters q, T, N and β can affect the accuracy and efficiency of the presented method. The domains size and the value of q determine number of oscillations of the exact solution, so we choose T, N and β in such a way that we can achieve the most accurate results

for a given q.
The Gauss-Chebyshev nodes on $[0, T]$ are used as the collocation points for the NGCM and the CSCM. For many problems, a Chebyshev distribution of nodes is a good choice [30]. Also we use the Legendre-Gauss nodes for the LSCM.
We need the following criterions for studying the convergence behavior of the presented method.

(i) Absolute error:
$$\mathrm{Abr} = |y(t) - y_N(t)|,$$
(ii) The point-wise L_∞ error:
$$L_N = \mathrm{Max}_{i=0}^{N}\{\mathrm{Abr}(t_i)\},$$
where $\{t_i\}_{i=0}^{N}$ is the set of collocation points.
(iii) The condition number of the coefficient matrix of the discretization method:
$$K_s(A) = \|A\|_s \cdot \|A^{-1}\|_s, \quad s = 2, \infty.$$

All computations are run on a Microsoft PC 32-bit AMD, Dual Core with 2.70 GHz of CPU and 4GB RAM. Also we use Maple 18 software for solving the linear algebraic systems directly by the LinearSolve command. In addition, for counteracting influence of rounding errors all calculations are performed using 50 digits precision.

Example 4.1. For the first example we consider the following PVIDE
$$y'(t) = g(t) + \mathrm{Cos}(t)y(t) + \mathrm{Sin}(t)y(qt) + \int_0^t tsy(s)ds + \int_0^{qt}(t-s)y(s)ds, \quad t \in [0, T], \tag{4.1}$$
where
$$g(t) = \frac{\mathrm{Cos}(\frac{t}{q})}{q} - \mathrm{Cos}(t)\mathrm{Sin}\big(\frac{t}{q}\big) - \mathrm{Sin}^2 t - q^2 t\mathrm{Sin}t - q^2 t\mathrm{Sin}\big(\frac{t}{q}\big) + qt^2\mathrm{Cos}\big(\frac{t}{q}\big) - qt - q^2 t\mathrm{Cos}(t) + q^2\mathrm{Sin}t + qt\mathrm{Cos}(t),$$
and the exact solution is $\mathrm{Sin}\big(\frac{t}{q}\big)$.

At first we let $q = 1$ and $T = \pi$ and solve eq. (4.1) using the standard Gaussian collocation method (SGCM), the standard inverse multiquadrid collocation method (SIMCM) and the NGCM. We compare the methods for different values of N. We increase c for the standard methods. Therefor from the relation $\beta = \frac{2T}{Nc^2}$, β varies with N for

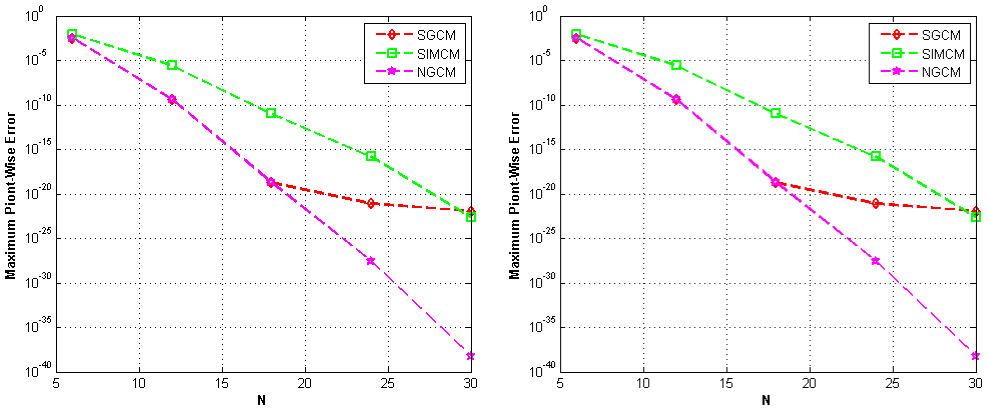

(A) $L_N(y_N)$ (B) $L_N(y'_N)$

FIGURE 1. Comparision between standard RBF methods and NGCM for $T = \pi$ and $q = 1$.

the NGCM. By using this relation we compare the NGCM and the SGCM, specifically. Numerical results are displayed in Table 1, fig. 1 .The results show that the convergence rate of NGCM is much faster than the standard methods. Also we see that the condition number which relates to the standard methods grows rapidly that is not the case for the NGCM. Moreover we observe an instable manner in the SGCM as N and c increase. The situation gets worse for the standard methods when $q < 1$. The convergence does not happen due to severe ill-conditioning of the standard methods. The ill-conditioning makes them too sensitive to small changes in q. if we let $T \leq 1$ for a given q near to 1 and $T \leq 0.5$ for $q \leq 0.5$ the results get better to some extent, but even in these cases the exponential convergence can not be obtained and the results are very poor. Perhaps if we apply an appropriate expensive technique to overcome the ill-conditioning, performance of the standard methods gets better, however with the NGCM without using any technique we can achieve excellent results even if we let $q \leq 0.1$.

Now we solve equ. (4.1) with the NGCM for $q = 0.1$ where $T = \pi$ and $\beta = 0.5$, also for $q = 0.1$ where $T = \pi$ and β varies with N and compare the results with those obtained with the LSCM and the CSCM. The obtained results are shown in Table 2 for different values of N. We observe that for the NGCM when we vary β with N the pointwise L_∞ error decreases more rapidly than while the β is fixed. Also

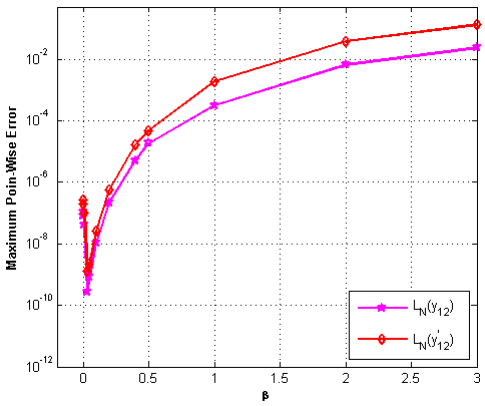

FIGURE 2. Behavior of the NGCM in terms of the point-wise L_∞ error versus β for $N = 12$, $q = 0.5$ and $T = \pi$

it can be seen that the NGCM gives better results than the spectral method while the condition number is relatively small and does not grow in like manner to the spectral method. For the spectral method we run the Maple program several times to obtain the results, whereas the exponential convergence is achievable easily by using the NGCM with relatively large N. So, one can conclude that the spectral method is more sensitive than the NGCM with respect to q.
Next, we apply the NGCM to approximate the solution of equ. (4.1) for fixed $N = 18$ and different values of β when $q = 0.1$ and $T = \pi$. The numerical results are shown in Table 3. Also fig. 2 displays the behavior of the NGCM in terms of the point-wise L_∞ error versus β for $N = 12$, $q = 0.5$ and $T = \pi$. Actually we use the Trial & Error technique which is composed of varying β and selecting the optimal parameter as the one that causes the minimum point-wise L_∞ error. It can be seen from Table 3 and the figure that one can improve the accuracy without extra computations.

TABLE 1. Comparision between standard RBF methods and NGCM for $T = \pi$ and $q = 1$.

		SMQCM				SGCM					NGCM			
N	C	$L_N(y_N)$	$L_N(y'_N)$	Cond_2	Cond_∞	$L_N(y_N)$	$L_N(y'_N)$	Cond_2	Cond_∞	β	$L_N(y_N)$	$L_N(y'_N)$	Cond_2	Cond_∞
6	2	$1.21e-2$	$3.21e-2$	10^8	$3e+8$	$3.27e-3$	$8.72e-3$	$2e+8$	$7e+8$	0.262	$3.27e-3$	$8.72e-3$	9435	32499
12	3	$2.98e-7$	$7.68e-7$	$3e+14$	$1e+15$	$3.88e-10$	$1.03e-9$	$6e+20$	$3e+21$	0.058	$3.88e-10$	$1.03e-9$	11043	44780
18	4	$1.54e-11$	$4.11e-11$	$3e+24$	$1e+25$	$1.85e-19$	$4.88e-19$	$2e+38$	$1e+39$	0.022	$1.85e-19$	$4.88e-19$	11047	46417
24	5	$3.58e-17$	$9.49e-17$	$1e+36$	$6e+36$	$7.57e-22$	$1.97e-21$	$6e+51$	$3e+52$	0.010	$2.66e-28$	$7.09e-28$	11048	47038
30	6	$2.80e-22$	$7.72e-22$	$8e+48$	$5e+49$	$1.13e-22$	$3.15e-22$	$2e+52$	$6e+52$	0.006	$6.24e-39$	$1.67e-38$	11048	47337

TABLE 2. Comparision between spectarl method and NGCM when $q = 0.1$, $T = \pi$ and β varies with N.

	LSM				CSM					NGCM				NGCM ($\beta = 0.5$)	
N	$L_N(y_N)$	$L_N(y'_N)$	Cond_2	Cond_∞	$L_N(y_N)$	$L_N(y'_N)$	Cond_2	Cond_∞	β	$L_N(y_N)$	$L_N(y'_N)$	Cond_2	Cond_∞	$L_N(y_n)$	$L_N(y'_N)$
18	$1.03e-1$	$3.00e-1$	2202	10164	$5.95e-2$	$1.48e-1$	2382	10455	0.5	$3.42e-4$	$1.01e-3$	2380	10453	$3.42e-4$	$1.01e-3$
24	$9.20e-5$	$2.76e-4$	2247	10434	$6.75e-4$	$1.78e-3$	2383	10611	0.4	$1.90e-7$	$4.95e-7$	2384	10611	$4.98e-7$	$7.03e-7$
30	$5.98e-8$	$2.04e-7$	2274	10567	$2.49e-7$	$6.67e-7$	2384	10686	0.3	$2.34e-11$	$5.11e-11$	2385	10685	$1.52e-9$	$2.39e-9$
36	$1.07e-11$	$3.76e-11$	2293	10643	no conv.	non conv.	-	-	0.2	$3.48e-16$	$8.95e-16$	2385	10728	$8.21e-12$	$2.21e-11$
42	no conv.	nov conv.	-	-	no conv.	no conv.	-	-	0.1	$2.07e-22$	$1.47e-21$	2385	10753	$6.38e-14$	$2.27e-13$

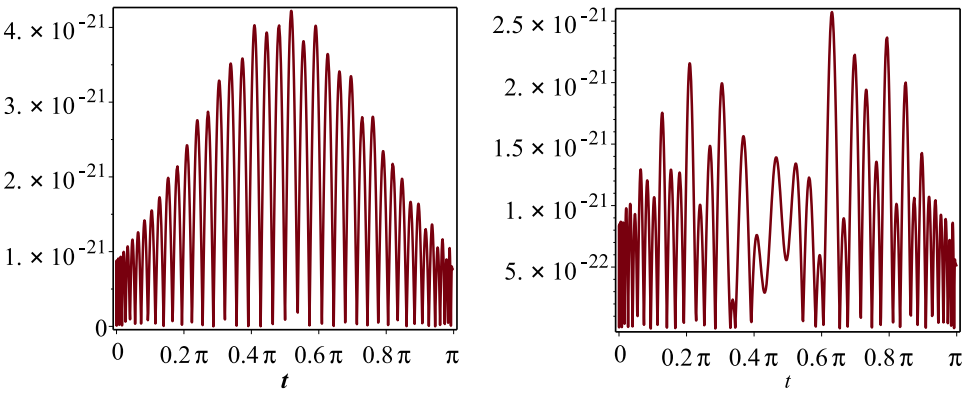

(A) $Abr(y_N)$ (B) $Abr(y'_N)$

FIGURE 3. Absolute errors for $N = 42$, $q = 0.1$, $\beta = 0.1$ and $T = \pi$

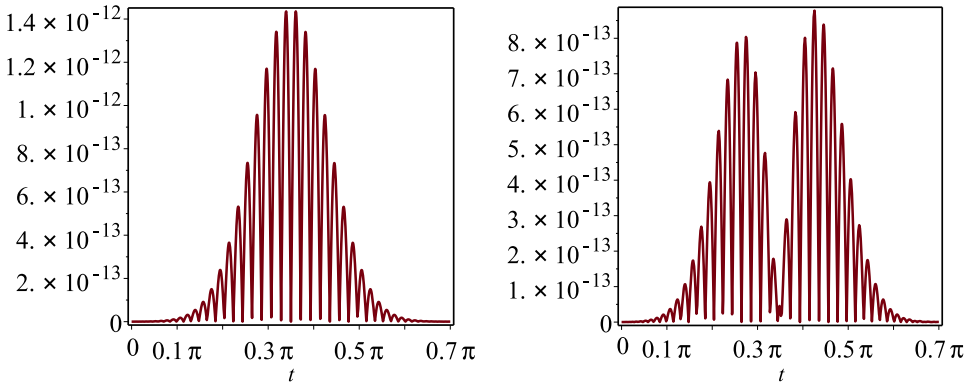

(A) $Abr(y_N)$ (B) $Abr(y'_N)$

FIGURE 4. Absolute errors for $N = 50$, $q = 0.05$, $\beta = 0.8$ and $T = 0.7\pi$.

TABLE 3. Numerical results of ex.1 when $N = 18$, $q = 0.1$, $T = \pi$ and different β.

β	3	2	1	0.5	0.3	0.1	0.05	0.01	0.003	0.00005
$L_N(y_N)$	$7.29e-1$	$3.01e-2$	$1.69e-3$	$3.97e-4$	$2.03e-3$	$1.85e-2$	$2.95e-2$	$4.39e-2$	$4.72e-2$	$4.87e-2$
$L_N(y'_N)$	$5.50e-1$	$9.60e-2$	$3.65e-3$	$9.74e-4$	$5.08e-3$	$3.00e-2$	$4.94e-2$	$7.92e-2$	$8.65e-2$	$8.97e-2$
$Cond_2$	12262	3670	2379	2380	2381	2381	2381	2381	2381	2381
$Cond_\infty$	45935	15331	10451	40453	10454	10455	10455	10455	10455	10455

In order to show the high performance of the NGCM on the whole domain, we plot the absolute errors for $N = 42$, $q = 0.1$, $\beta = 0.1$ and $T = \pi$ in fig. 3 . Also fig. 4 presents the absolute errors for $N = 50$, $q = 0.05$, $\beta = 0.8$ and $T = 0.7\pi$.

Example 4.2. The second example is as follow

$$y'(t) = g(t) + ty(t) + e^{-q^2t}y(qt) + \int_0^t \mathrm{Cos}\big(q(t-s)\big)y(s)ds + \int_0^{qt} q(t-s)y(s)ds, \quad t \in [0,T], \tag{4.2}$$

where $g(t)$ is given such that the exact solution to be $e^{qt}\mathrm{Cos}\big(\frac{t}{q}\big)$.
At first we solve this example for $q = 0.01$ and $\beta = 0.7$ where T is $\frac{\pi}{4}$ and $\frac{\pi}{5}$ to verify impact of the domains size on the accuracy of the presented method, where the variation of T is only 0.157. The results for different values of N are displayed in fig. 5. We see that for the smaller value of T the results are more accurate. Also in order to see how susceptible the GNCM is to the selection of β, we solve the equ. (4.2) for $q = 0.01$, $\beta = 1.5$ and $T = \frac{\pi}{5}$ and compare the results with those obtained for $\beta = 0.7$, which is depicted in fig. 6. In addition for $q = 0.01$, $\beta = 1.5$, $T = \frac{\pi}{5}$ and $N = 55$ we compare the numerical results y_N and y'_N and the exact solutions y and y' which are shown in fig. 7. Furthermore the absolute error of y_N and y'_N are plotted in fig. 8 respectively. These results show the flexibility and capability of the NGCM for solving such oscillatory problem with high oscillation. However the spectral method fails to converge when $q = 0.01$ and $T = \frac{\pi}{5}$. Although for $T \leq \frac{\pi}{7}$ the situation gets better but the obtained results are poor and the exponential convergence can not be acquired. Next, for $q = 0.09$ and $T = \pi$ we solve the equ. (4.2), when β varies with N. The numerical results are reported in Table 4. From the Table it can be seen that the exponential convergence is achievable. A comparison between the exact solutions and the numerical solutions when $N = 52$ and $\beta = 0.4$ is depicted in fig. 9.

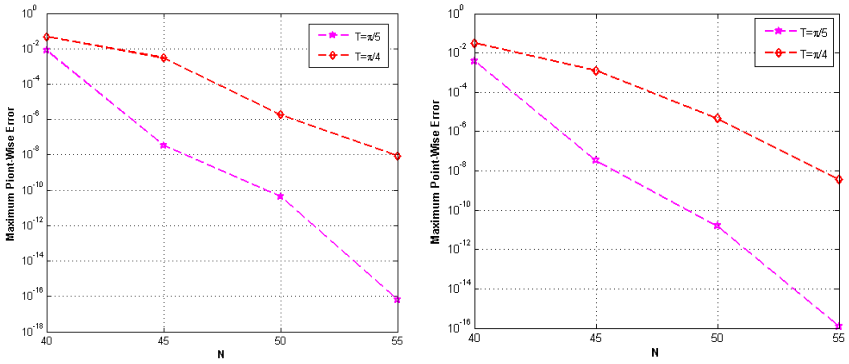

(A) $L_N(y_N)$ (B) $L_N(y'_N)$

FIGURE 5. Behavior of the NGCM in terms of the point-wise L_∞ error versus N for $q = 0.01$ and $\beta = 0.7$.

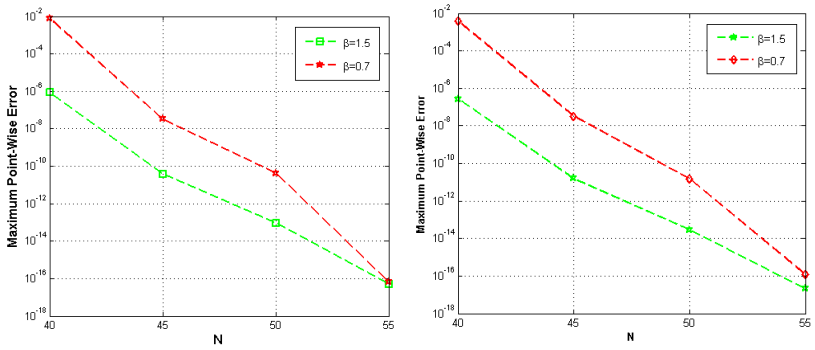

(A) $L_N(y_N)$ (B) $L_N(y'_N)$

FIGURE 6. Behavior of the NGCM in terms of the point-wise L_∞ error versus N for $q = 0.01$ and $T = \frac{\pi}{5}$.

TABLE 4. Numerical results of ex.2 when β varies with N and $q = 0.09$, $T = \pi$.

N	16	22	28	34	40	46	52
β	1	0.9	0.8	0.7	0.6	0.5	0.4
$L_N(y_N)$	$1.69e-1$	$2.75e-4$	$7.68e-6$	$3.60e-8$	$6.38e-11$	$2.05e-14$	2.67e18
$L_N(y'_N)$	$5.90e-1$	$7.50e-4$	$1.25e-5$	$7.23e-8$	$9.23e-11$	$4.66e-14$	$5.20e-18$
$Cond_2$	11737	11921	11984	12209	12689	12862	12692
$Cond_\infty$	42300	42075	43917	49038	52749	51762	50109

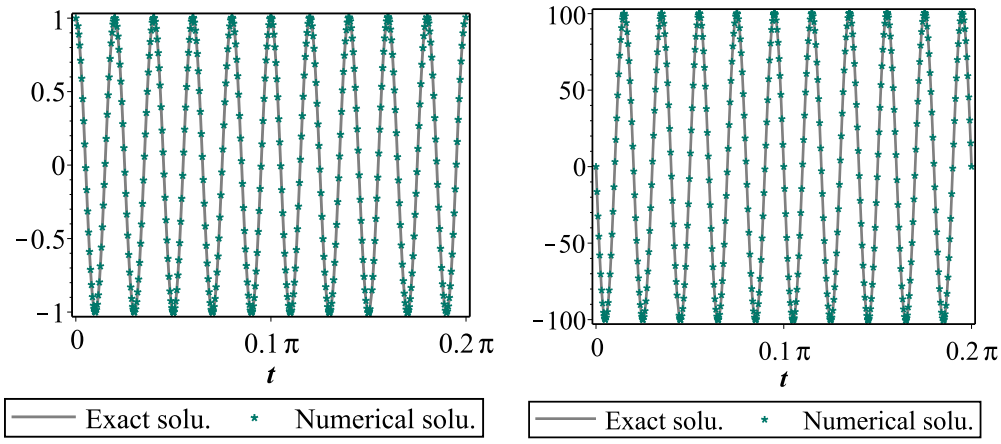

(A) $y(t)$ (B) $y'(t)$

FIGURE 7. Comparision of Numerical solutions and exact solutions when $q = 0.01$, $T = \frac{\pi}{5}$, $\beta = 1.5$ and $N = 55$

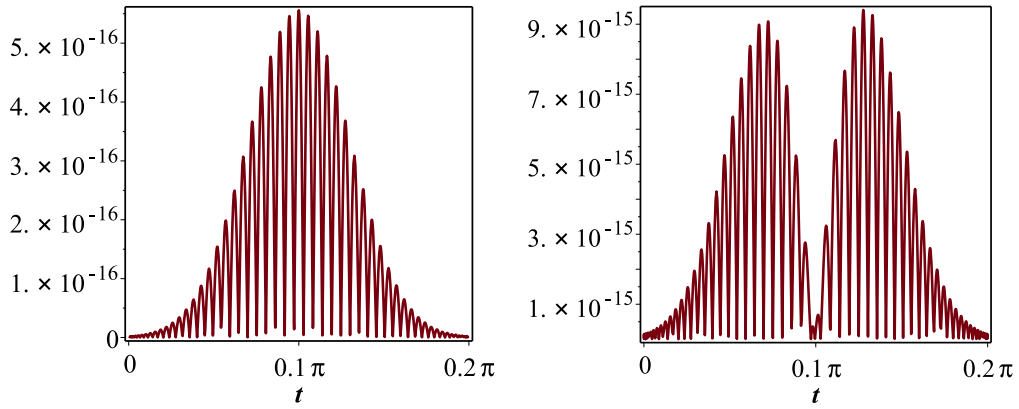

(A) $Abr(y_N)$ (B) $Abr(y'_N)$

FIGURE 8. Absolute errors for $q = 0.01$, $T = \frac{\pi}{5}$, $\beta = 1.5$ and $N = 55$.

5. Conclusion

In this paper we use a simple explicit interpolation formula based on GRBF with equally spaced centers to establish a stable collocation method for solving the PVIDEs. By this method we overcome the ill-conditioning of the interpolation matrix, without applying a special technique. Numerical results show that the efficiency and stability of

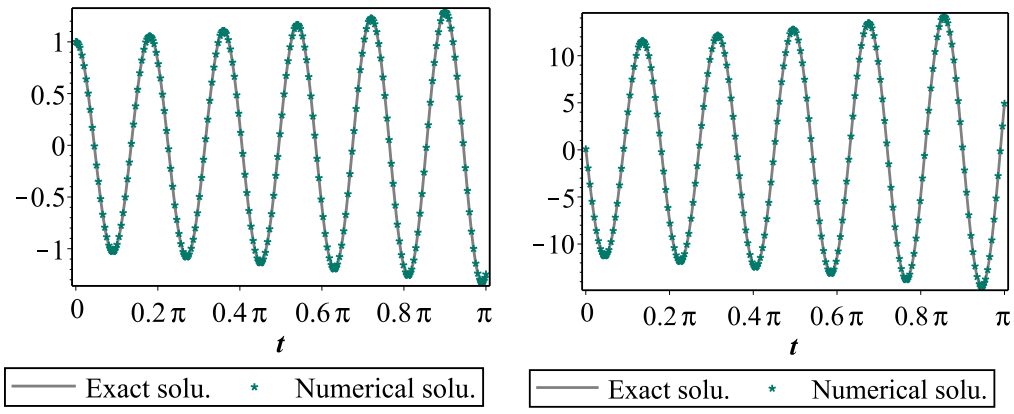

(A) $y(t)$ (B) $y'(t)$

FIGURE 9. Comparision of Numerical solutions and exact solutions when $q = 0.09$, $T = \pi$, $\beta = 0.4$ and $N = 52$

the presented method is excellent with respect to standard method especially when $q < 1$. While comparing with the spectral method, the NGCM shows better performance and it can be seen that the spectral method is more sensitive than the NGCM with respect to q. Also the exponential convergence of the presented method is achievable easily even for relatively small value of q and relatively large N, however that is not the case for the spectral method. Furthermore one can improve the accuracy of the NGCM without extra computation while β decreases. So the NGCM is a robust method for solving the PVIDEs which is motivated us to extend it for solving more complicated problems such as fractional pantograph partial integro-differential equations that remains for future works.

REFERENCES

[1] M.D. Buhmann, Radial Basis Function Cambridge, Cambridge University Press, 2003.

[2] E.J. Kansa, Muliquadrics scattered data approximation scheme with applications to computational fluid dynamics: II. Solutions to parabolic, hyperbolic, and elliptic partial differential equations, Comput. Math. Appl. 19 (1990) 147161.

[3] W.R. Madych, S.A. Nelson, Bounds on multivariate interpolation and exponential error estimates for multiquadric interpolation, J. Approx. Theory 70 (1992) 94114.

[4] B.-C. Shin and J.-H. Jung, Spectral collocation and radial basis function methods for one-dimensional interface problems, Applied Numerical Mathematics, vol. 61, no. 8, pp. 911928, 2011.

[5] Fornberg, Bengt, and Grady Wright. "Stable computation of multiquadric interpolants for all values of the shape parameter." Computers & Mathematics with Applications 48.5 (2004): 853-867.
[6] Driscoll, Tobin A., and Bengt Fornberg. "Interpolation in the limit of increasingly flat radial basis functions." Computers & Mathematics with Applications 43.3 (2002): 413-422.
[7] Fasshauer, Gregory E., and Jack G. Zhang. "Preconditioning of radial basis function interpolation systems via accelerated iterated approximate moving least squares approximation." Progress on Meshless Methods. Springer Netherlands, 2009. 57-75.
[8] Platte, Rodrigo B. "How fast do radial basis function interpolants of analytic functions converge?." IMA journal of numerical analysis (2011): drq020..
[9] Platte, Rodrigo B., and Tobin A. Driscoll. "Polynomials and potential theory for Gaussian radial basis function interpolation." SIAM Journal on Numerical Analysis 43.2 (2005): 750-766.
[10] Parand, K., et al. "A novel application of radial basis functions for solving a model of first-order integro-ordinary differential equation." Communications in Nonlinear Science and Numerical Simulation 16.11 (2011): 4250-4258.
[11] Alipanah, Amjad, and Shahrokh Esmaeili. "Numerical solution of the two-dimensional Fredholm integral equations using Gaussian radial basis function." Journal of computational and applied mathematics 235.18 (2011): 5342-5347.
[12] Parand, K., and J. A. Rad. "Numerical solution of nonlinear VolterraFredholmHammerstein integral equations via collocation method based on radial basis functions." Applied Mathematics and Computation 218.9 (2012): 5292-5309.
[13] Tohidi, E., A. H. Bhrawy, and Kh. Erfani. "A collocation method based on Bernoulli operational matrix for numerical solution of generalized pantograph equation." Applied Mathematical Modelling 37.6 (2013): 4283-4294.
[14] Bhrawy, Ali H., et al. "A Legendre-Gauss collocation method for neutral functional-differential equations with proportional delays." Advances in Difference Equations 2013.1 (2013): 1-16.
[15] H. Brunner, Collocation Methods for Volterra Integral and Related Functional Equations, Cambridge University Press, Cambridge, 2004.
[16] Doha, E. H., et al. "A new Jacobi rationalGauss collocation method for numerical solution of generalized pantograph equations." Applied Numerical Mathematics 77 (2014): 43-54.
[17] Yzba, uayip. "An efficient algorithm for solving multi-pantograph equation systems." Computers & Mathematics with Applications 64.4 (2012): 589-603.
[18] Yzba, uayip, and Mehmet Sezer. "Shifted Legendre approximation with the residual correction to solve pantograph-delay type differential equations."Applied Mathematical Modelling (2015).
[19] Yzba, uayip, and Mehmet Sezer. "An exponential approach for the system of nonlinear delay integro-differential equations describing biological species living together." Neural Computing and Applications (2015): 1-11.
[20] I. Ali, H. Brunner and T. Tang, Spectral methods for pantograph-type differential and integral equations with multiple delays, Front. Math. China, 4 (2009), 49-61.

[21] Baker, Christopher TH, Christopher AH Paul, and David R. Will. "Issues in the numerical solution of evolutionary delay differential equations." Advances in Computational Mathematics 3.3 (1995): 171-196.

[22] Brunner, Hermann, and Qiya Hu. "Optimal superconvergence results for delay integro-differential equations of pantograph type." SIAM Journal on Numerical Analysis 45.3 (2007): 986-1004.

[23] Ali, Ishtiaq. "Convergence analysis of spectral methods for integro-differential equations with vanishing proportional delays." J. Comput. Math29 (2011): 49-60.

[24] Wei, Yunxia, and Yanping Chen. "Legendre spectral collocation method for neutral and high-order Volterra integro-differential equation." Applied Numerical Mathematics 81 (2014): 15-29.

[25] Yoon, Jungho. "Spectral approximation orders of radial basis function interpolation on the Sobolev space." SIAM journal on mathematical analysis33.4 (2001): 946-958.

[26] Dehghan, Mehdi, and Ali Shokri. "A meshless method for numerical solution of the one-dimensional wave equation with an integral condition using radial basis functions." Numerical Algorithms 52.3 (2009): 461-477.

[27] Davis, Philip J. Interpolation and approximation. Courier Corporation, 1975.

[28] Fornberg B. A practical guide to pseudospectral methods. Cambridge university press; 1998.

[29] Yang, Yin, and Yunqing Huang. "Spectral-collocation methods for fractional pantograph delay-integrodifferential equations." Advances in Mathematical Physics 2013 (2013).

[30] Kormann, Katharina, and Elisabeth Larsson. An RBF-Galerkin approach to the time-dependent Schrdinger equation. Technical report 2012-024, Department of Information Technology, Uppsala University, Uppsala, Sweden, 2012.